

Article

Effect of Bulk Nanobubbles on the Flocculation and Filtration Characteristics of Kaolin Using Cationic Polyacrylamide

Yihong Li ^{1,2}, Guangxi Ma ³, Muhammad Bilal ⁴ , Jie Sha ^{1,2,*} and Xiangning Bu ^{1,*} 

¹ School of Chemical Engineering and Technology, China University of Mining & Technology, Xuzhou 221116, China; kjliyhong@163.com

² Shaanxi Xinneng Coal Preparation Technology Co., Ltd., Xi'an 710100, China

³ School of Resources and Environmental Engineering, Shandong University of Technology, Zibo 255049, China; sdut_mgx@sdut.edu.cn

⁴ Department of Mining Engineering, Balochistan University of Information Technology, Engineering and Management Sciences (BUIITEMS), Quetta 87300, Pakistan; bilalkhan4p@gmail.com

* Correspondence: shajie@cumt.edu.cn (J.S.); xiangning.bu@foxmail.com (X.B.)

Abstract: This study investigated the influence of bulk nanobubbles (NBs) on the flocculation and filtration behavior of kaolin suspensions treated with cationic polyacrylamide (CPAM). Traditionally, flocculation relies on bridging mechanisms by polymers like CPAM. The present work examines the possibility of combining NBs with CPAM to achieve more efficient kaolin separation. The settling behavior of kaolin suspensions with and without bulk nanobubbles was compared. The results with 2 mL CPAM and 300 s settling time revealed that bulk NBs significantly enhanced flocculation efficiency, with supernatant zone height reductions exceeding 50% compared to CPAM alone, indicating a faster settling rate resulting from bulk NBs. This improvement in the settling rate is attributed to NBs' ability to reduce inter-particle repulsion (as evidenced by a shift in zeta potential from -20 mV to -10 mV) and bridge kaolin particles, complementing the action of CPAM. Additionally, the study demonstrated that bulk NBs improved dewatering characteristics by lowering the medium resistance and specific cake resistance during filtration. These findings pave the way for the utilization of bulk NBs as a novel and efficient strategy for kaolin separation in mineral processing, potentially leading to reduced processing times and lower operational costs.

Keywords: bulk nanobubbles; kaolin; flocculation; dewatering; cationic polyacrylamide; flocculation



Citation: Li, Y.; Ma, G.; Bilal, M.; Sha, J.; Bu, X. Effect of Bulk Nanobubbles on the Flocculation and Filtration Characteristics of Kaolin Using Cationic Polyacrylamide. *Minerals* **2024**, *14*, 405. <https://doi.org/10.3390/min14040405>

Academic Editor: Cyril O'Connor

Received: 11 March 2024

Revised: 3 April 2024

Accepted: 12 April 2024

Published: 15 April 2024



Copyright: © 2024 by the authors. Licensee MDPI, Basel, Switzerland. This article is an open access article distributed under the terms and conditions of the Creative Commons Attribution (CC BY) license (<https://creativecommons.org/licenses/by/4.0/>).

1. Introduction

Clay minerals, such as kaolin, montmorillonite, and illite, are commonly found in the flotation tailings of mineral processing plants [1,2]. Their fine particle size and strong electronegativity make them stable colloids, hindering aggregation and settling [3,4]. Coagulation–flocculation, a well-established physico-chemical method in industries, destabilizes these dispersed particles [5,6]. This method works by reducing electrostatic interaction energy, often achieved by adding salt ions, as explained by DLVO theory [7,8].

Efficient flocculants are crucial for clay settling as they promote the formation of large flocs [9]. Synthetic polymers such as cationic (CPAM), anionic (APAM), and nonionic polyacrylamide (NPAM) are commonly used flocculants in wastewater treatment of mineral processing and papermaking. While these polymers effectively form large and strong clay flocs, compared to APAM and NPAM, CPAM can produce a faster sedimentation rate of coal slurry [10]. The cationic polymer flocculants have the dual functions of aggregation and flocculation. The effectiveness of CPAM is attributed to the high charge density, the large molecular weight, and the long molecular chain [11]. Compared with natural polymers, these synthetic polymers are non-biodegradable, expensive, and can sometimes cause health hazards [12,13]. Recent research focuses on developing environmentally friendly alternatives like starch, chitosan, pomegranate seed powder, and cellulose due to

their biodegradability and renewability [14–20]. However, compared to synthetic polymer flocculants, natural flocculants exhibit poorer stability, poorer bridging performance, and high required therapeutic dose [21–23]. To further improve the effectiveness of natural flocculants, physical or chemical modifications like gelatinization, etherification, esterification, and grafting have been used to create environmentally friendly starch-modified flocculants [24–26]. Compared to unmodified flocculants, starch-modified flocculants have a macromolecule network with excellent properties from both starch and acrylamide, leading to wider molecular chains, good thermal stability, and improved flocculation performance for wastewater treatment [27,28].

Flocculant addition generally enhances floc formation through charge neutralization, bridging effects, or a combination of both, ultimately improving kaolin dewatering performance [29,30]. There is a close relationship between flocculation and filtration processes. Generally, the larger the floc formed, the faster the floc settling rate. However, excessively large flocs can trap a large amount of water in the filter cake, leading to a deterioration of the filtration effect [31]. Pre-treatments like ultrasonic and hydrodynamic cavitation can further promote dewatering. The experimental results showed that with an increase in the treatment time of ultrasonic and hydrodynamic cavitation, the viscosity of flocculants decreases gradually and a flocculant mixture system with multimolecular weight is formed. These modified flocculants have been shown to create smaller and tighter flocs, reducing total dewatering resistance, and increasing filter cake porosity [22,31,32].

Nanobubbles (NBs) possess unique physicochemical properties, including large specific surface area, low terminal velocity, and long lifetimes, making them attractive for enhancing mineral flotation [33,34]. It is important to note that some of the literature defines NBs as both micro-scale and nano-scale bubbles [35–37]. Furthermore, there are two types of NBs used in mineral flotation: bulk and surface NBs [38–41]. Diniz, et al. [42] reported that bulk NBs can reduce the filtration time of a quartz suspension due to their enhancement effect on the hydrophobized quartz (using a dodecyl-ether-amine before filtration tests).

Researchers have observed the attachment of hydrophilic particles to bulk nanobubbles [43–46]. This attachment can lead to a more porous coagulation type in the early stages of the flocculation of kaolinite suspensions [45]. Hydrophobic forces, repulsive van der Waals, hydrogen bonds, and electrical double-layer (EDL) forces may contribute to the attachment between a hydrophilic solid and a bubble [47–49]. In conclusion, the presence of bulk NBs can promote the formation of flocs and the filtration of kaolin. However, the influence of bulk NBs on the kaolin flocculation and filtration processes in the presence of flocculants is yet to be investigated further.

However, there is a lack of literature on the application of bulk NBs in flocculation and cake filtration involving kaolin. Meanwhile, there is no study on the effect of bulk NBs on the flocculation, sedimentation, and dewatering processes of hydrophilic minerals, mainly clay minerals. This study aims to address this gap by evaluating the effects of CPAM concentrations on flocculation and dewatering performance with and without bulk NBs. The floc size, turbidity, zeta potential, and low-field nuclear magnetic resonance measurements were used to understand the mechanism of bulk NBs on kaolin filtration and dewatering characteristics. Furthermore, the findings of this research could contribute to the development of more efficient and environmentally friendly methods for clay processing in mineral processing plants.

2. Materials and Methods

2.1. Materials

The kaolin sample (d_{50} : 2.32 μm) was purchased from the Hongtu Mining Company (Zhaoping, China). CPAM ($[-\text{CH}_2\text{CH}(\text{CONH}_2)-]_x$, 1200 million g/mol) was obtained from Tianjin Zhiyuan Chemical Reagent Co., Ltd. (Tianjin, China).

2.2. Experimental Procedure

2.2.1. Preparation of Bulk NBs

The bulk NBs were generated using a GWN micro-nanobubble preparation machine (GWN-0.31, Gongyuan Environment company, Wuxi, China). The machine was set to an airflow rate of 60 mL/min and a preparation time of 10 min. To eliminate any unstable microbubbles, the milky solution was left for 10 min. A similar procedure for obtaining bulk nanobubble water can be found in the literature [40]. The size of the bulk nanobubbles was determined using nanoparticle tracking analysis (Nanosight-NS300, Malvern Panalytical Ltd., Malvern, UK), which varied between 50 to 200 nm. The bubble concentration was measured to be $3.1 \times 10^8 \text{ mL}^{-1}$.

2.2.2. Flocculation and Dewatering Tests

To prepare 0.1% *w/v* concentration CPAM solutions for flocculation and dewatering tests, ultrapure water and bulk nanobubble water were used, respectively. Ultrapure water with a conductivity of about 18.2 M Ω ·cm was produced using the Easy-2-15 (Heal Force, Shanghai, China) water purification system and was employed for all experimental tests. Five grams of kaolin particles were dispersed in 250 mL of pure water or bulk nanobubble water using a magnetic stirrer at 1000 r/min for 4 min. The kaolin suspension was then treated with different volumes of CPAM solution (0.5–12 mL) and stirred for 2 min. The kaolin suspension was transferred to a 250 mL graduated cylinder for flocculation studies, and the height of the clarification zone was recorded after the cylinder was turned over five times.

A Buchner funnel-type vacuum filtration unit was used for the dewatering studies. The kaolin suspension was filtered through a Buchner funnel, and the filtrate volume was measured in a graduated cylinder at regular intervals. The pore-size distribution of the filter cake was further analyzed using a low-field nuclear magnetic resonance (NMRC12-010V, Niumag Corporation, Suzhou, China).

Filtration rate, cake permeability, and specific cake resistance were calculated using the integrated form of Darcy's equation under conditions of constant pressure and cake permeability [50]. The equation is given as follows:

$$\frac{t}{V} = \frac{\alpha\mu c}{2A^2\Delta P}V + \frac{R_m\mu}{A^2\Delta P} \quad (1)$$

where *t* and *V* represent the filtration time and filtrate volume, respectively, and *c*, μ , α , and ΔP are the slurry concentration (0.002 kg/m³), absolute viscosity of water (0.001 Ns/m²), filter cake area (0.0104 m²), and differential pressure (0.100 N/m²), respectively.

2.3. Analytical Methods

2.3.1. Zeta Potential Measurement

A Brookhaven Zeta Plus Zeta potential meter (Zeta Plus, Brookhaven, Holtsville, NY, USA) was used to carry out the zeta potential measurement as per standard procedures. A sample with a solid concentration of 0.02% was introduced into a 100 mL beaker. The supernatant from the kaolin suspension, following a settlement period of 2 min, was utilized for the measurement of zeta potential. Each experiment was repeated five times, and the average was considered the final value.

2.3.2. Polarizing Microscopy Observation

A polarizing microscope (Sunny Optical-Instrument, Yuyao, China) was utilized to observe the flocs after the settlement process. A small quantity of the sample was removed from the graduated cylinder and placed on a dry glass slide, which was then examined under the polarizing microscope. In the zeta potential test, the pH was adjusted using sodium hydroxide and hydrochloric acid. The pH of the solution in polarizing microscopy observation remained unchanged and was approximately 6.8, which is the pH of pure

water. Details of the zeta potential measurement and polarizing microscopy observation can be found in the literature [33,51].

2.3.3. DLVO Theory Calculation Process

To calculate the DLVO interactions, the zeta potential values under the flocculant dosage of 6 mL and the kaolin particle size of 2.32 μm (d_{50}) were used. The equations for van der Waals potential energy (E_A), electrostatic potential energy (E_E), and the total potential energy (E_T) are as follows [52,53]:

$$E_T = E_W + E_E, \quad (2)$$

where E_T is the total interaction energy, E_W is the van der Waals interaction, E_E is the electrical double-layer interaction. The specific calculation process for each of these interactions is described in detail.

The van der Waals interaction (E_W) is calculated according to Equation (3):

$$E_W = -\frac{A_{132}R_1R_2}{6H(R_1R_2)}, \quad (3)$$

where H represents the distance between two spherical particles, R_1 and R_2 represent the radius of fine and coarse particles, and A_{132} is the Hamaker constant of the minerals 1 and 2 in the medium 3.

$$A_{132} \approx (\sqrt{A_{11}} - \sqrt{A_{33}})(\sqrt{A_{22}} - \sqrt{A_{33}}), \quad (4)$$

where A_{11} , A_{22} , and A_{33} are the Hamaker constants for mineral 1, mineral 2, and water (4.0×10^{-20} J) [54] in a vacuum, respectively. The Hamaker constant of kaolinite (A_{132}) in water is 4.68×10^{-21} J.

The electrical double-layer interaction (E_E) is calculated using Equation (5):

$$E_E = \frac{\pi\epsilon\epsilon_0R_1R_2}{R_1 + R_2}(\varphi_1^2 + \varphi_2^2) \left(\frac{2\varphi_1\varphi_2}{\varphi_1^2 + \varphi_2^2} \ln \left[\frac{1 + \exp(-\kappa H)}{1 - \exp(-\kappa H)} \right] + \ln[1 - \exp(-2\kappa H)] \right), \quad (5)$$

where ϵ_0 is the absolute dielectric constant in a vacuum (8.854×10^{-12} F/m), ϵ is the relative dielectric constant of the dispersion medium (for water, 78.5 F/m), κ is the Debye constant, φ_1 and φ_2 are the surface potential of mineral 1 and mineral 2 that are usually replaced by the zeta potential ξ . The Debye constant is considered as 3.33×10^8 m^{-1} for the electric double-layer interaction calculation [53]. The zeta potential values of the kaolin suspension in the absence and presence of bulk NBs were -7.90 and -4.69 mV, respectively.

3. Results

3.1. Flocculation Performance

The effects of bulk NBs on the height of the supernatant and the settling rates of the kaolin suspension at different CPAM dosages are illustrated in Figure 1. As can be observed in Figure 1, the height of the supernatant increases substantially with an increase in flocculant dosage, indicating a faster settling rate. The slope of the curve in Figure 1 is used to calculate the settlement velocity. The settling rate is the slope obtained by fitting a straight line. The increase in the settling rate with an increase in CPAM dosage is attributed to the increase in floc size due to the bridging effect of flocculants and bulk NBs. As the dosage of flocculant increases, more flocculant molecules connect free kaolin particles through adsorption bridging to form large aggregates [4,55]. However, it is important to note that an excessively high dosage of flocculant can weaken flocculation performance due to intermolecular interactions [25,56].

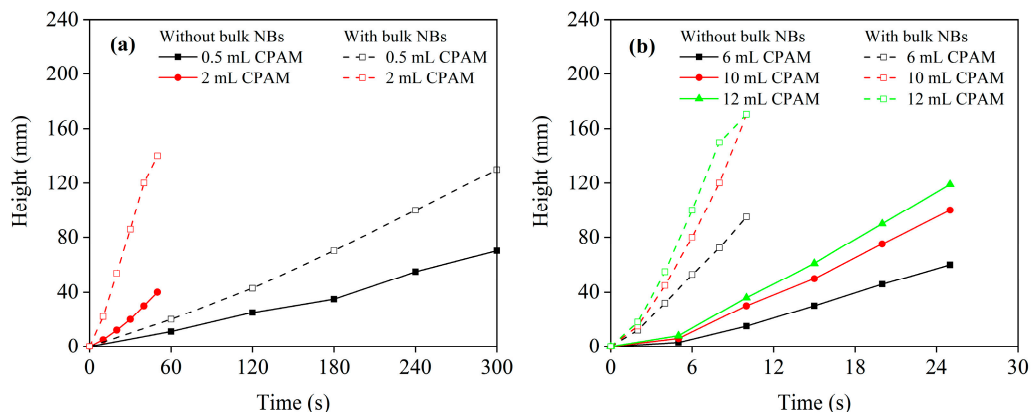


Figure 1. Effects of bulk NBs on supernatants' heights and settling rates of kaolin suspension under different CPAM dosages: (a) 0.5 and 2 mL CPAM; (b) 6, 10, and 12 mL CPAM.

As can be seen from Figure 2, the presence of bulk NBs results in a significant increase in the settling rate compared to that of without bulk NBs. The floc images under different flocculant dosages in the presence and absence of bulk NBs are given in Figure 3. The use of more kaolin particles to form larger flocs through the bridging effect with the help of bulk NBs can enhance the settling performance. This can be observed in the images of flocs under different CPAM concentrations in the absence and presence of bulk NBs (Figure 3). It is observed that bulk NBs lead to the formation of larger flocs compared to their absence.

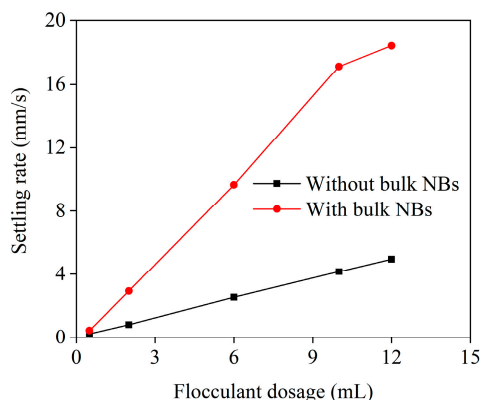


Figure 2. Settling rates of kaolin suspension under different CPAM dosages.

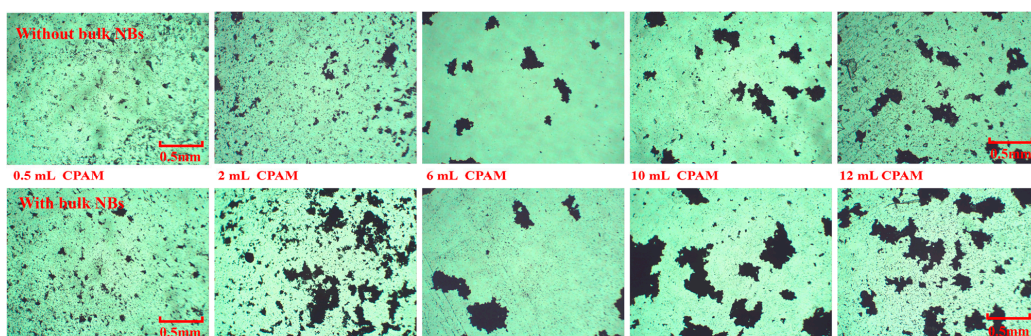


Figure 3. The floc images under different flocculant dosages in the absence and presence of bulk NBs.

The zeta potentials of kaolin particles in the absence and presence of bulk NBs are shown in Figure 4. The presence of bulk NBs in the CPAM solution preparation decreases the absolute value of the zeta potential of kaolin particles compared to the CPAM solution without bulk NBs. This decrease in zeta potential is beneficial in reducing the repulsive force between colloidal particles, facilitating the instability of the colloidal system and

promoting particle aggregation [57]. The DLVO interaction energy calculation results are presented in Figure 5. A negative value of the interaction energy stands for the attraction force between particles, while a positive value represents a repulsive force. The presence of bulk NBs has no impact on van der Waals interaction energy (E_W) due to the same Hamaker constants used in the study. However, the presence of bulk NBs significantly decreases the electrostatic interaction energy (E_E), resulting in a significant decrease in the total interaction energy (E_T) between kaolin particles. Therefore, the presence of bulk NBs in CPAM solution contributes to the occurrence of the flocculation of kaolin particles by increasing the attraction interaction energy between kaolin particles.

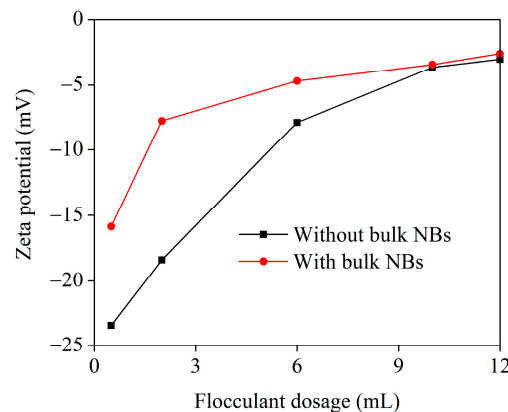


Figure 4. Zeta potentials of kaolin particles in the absence and presence of bulk NBs.

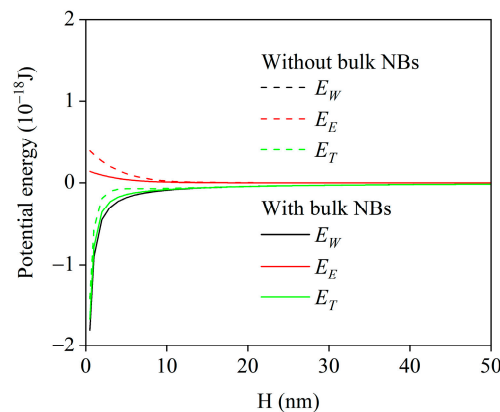


Figure 5. EDLVO interaction energy calculation results in the absence and presence of bulk NBs.

3.2. Dewatering Performance

The moisture contents of filter cake for different flocculant dosages with and without bulk NBs are shown in Figure 6. As the flocculant dosage increases, the moisture content of the filter cake rises for both cases both with and without NBs. This occurs because an increased flocculant dosage leads to the capture of excess water in the filter cake, resulting in a higher water content [58,59]. Moreover, a higher flocculant dosage leads to more flocculant molecules remaining in the water, which obstructs the pores within the filter cake and filter medium [22,60].

When the CPAM dosage is minimal, the presence of NBs does not significantly lower the moisture content of the filter cake. Under conditions of reduced flocculant dosage, the negative effect of NBs on the moisture content of the filter cake might be attributed to the floc structure formed by free NBs and kaolin particles. The results of sedimentation tests indicate that the presence of bulk NBs can lead to the formation of sediment with significantly lower density. This can be explained by the formation of flocs having edge-to-edge contacts stabilized by gas bubbles [44,45]. The production of long-range edge-to-edge (EE) attractive forces is attributed to the presence of bulk NBs. These forces aid in the

formation of a more porous coagulation structure, mainly characterized by EE particle configurations. This structure is more open than the structure with edge-to-face (EF) and face-to-face contacts, which are more compact [45,61]. The excess water is trapped within the smaller flocs formed due to the presence of bulk NBs, leading to the formation of these clay flocs.

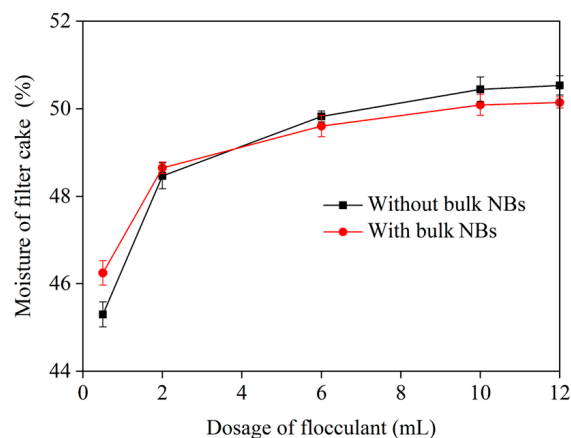


Figure 6. Filter cake moisture contents with different flocculant dosages in the absence and presence of bulk NBs.

However, when the CPAM dosage is greater than 4 mL, the presence of bulk NBs is beneficial for reducing the moisture content of the filter cake. The enhanced dewatering performance of bulk NBs can be attributed to their interaction with CPAM. As illustrated in Figure 3, the presence of bulk NBs results in larger floc sizes compared to their absence. Similarly, as seen in Figure 7, the presence of bulk NBs leads to the formation of less compact structures than when they are absent. This enhanced dispersion performance of the CPAM solution containing bulk NBs can be beneficial for the flocculation process of fine kaolin particles.

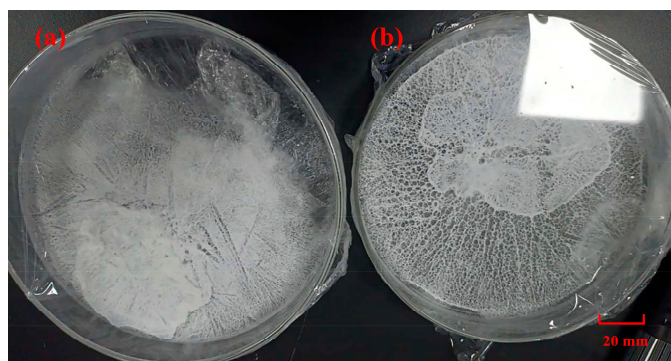


Figure 7. Images of CPAM solution prepared by lyophilization of the absence (a) and presence (b) of bulk NBs.

It is important to note that a relatively low dosage of CPAM can achieve a significant reduction in the absolute value of the zeta potential (Figure 4). This is due to the unique crystal structure of kaolinite, which has a point of zero charge (PZC) near pH 7 [62]. The surface charge of bulk NBs, which is approximately -20 to -35 mV, can be attributed to the adsorption of free radicals at the gas/liquid interface [40,63]. As a result, the coexistence of NBs with CPAM can cause a greater number of kaolin particles to flocculate leading to a reduction in the absolute value of the zeta potential.

A straight line is formed when plotting t/V against V , and the intercept on the y-axis indicates the value of medium resistance (R_m). Moreover, the slope of the line is utilized to calculate the specific cake resistance (α). There is a positive correlation between the slope

and specific cake resistance (α) [22]. The plots of t/V versus V data in the absence and presence of bulk NBs under 6 mL CPAM dosage are given in Figure 8. The corresponding values of R_m and α are listed in Table 1. The fitting model’s accuracy can be evaluated by the determination coefficient (R^2), which is greater than 0.80, indicating the practicality of the fitting result [64–67]. As demonstrated in Figure 8 and Table 1, the presence of bulk NBs in CPAM solutions can reduce the medium resistance from 4.0×10^{-8} to 3.6×10^{-8} and the specific cake resistance from 8.3×10^{-9} to 7.6×10^{-9} compared to the absence of bulk NBs.

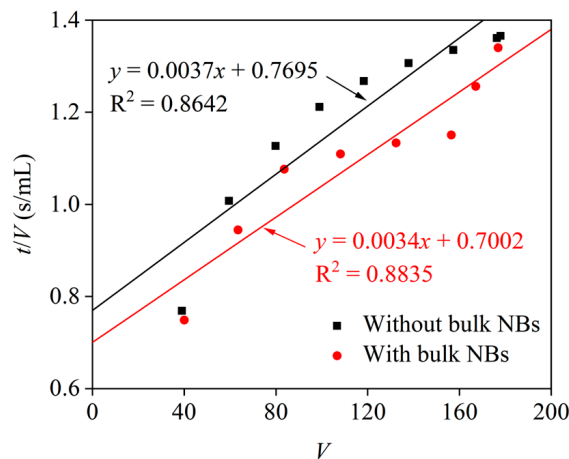


Figure 8. Plots of t/V versus V data in the absence and presence of bulk NBs under 6 mL CPAM dosage.

Table 1. The calculated results of R_m and α using Equation (1) in the absence and presence of bulk NBs.

Condition	Fitting Equation	α (m/kg)	R_m (m ⁻¹)	R^2
Without bulk NBs	$y = 0.0037x + 0.7695$	4.0×10^{-8}	8.3×10^{-9}	0.8642
With bulk NBs	$y = 0.0034x + 0.7002$	3.6×10^{-8}	7.6×10^{-9}	0.8835

The enhancement in the dewatering characteristics due to bulk NBs can be attributed to the higher flocculation efficiency. With the presence of bulk NBs, a larger number of kaolin particles contribute to the formation of flocs, increasing in floc size. The enlarged floc size enables an increase in the free water content between kaolin particles [68,69]. According to previous research [43–45], the presence of nanobubbles can promote the formation of aggregates between kaolin particles, which is beneficial for capturing more free and fine kaolin particles. As a result, the presence of nanobubbles leads to fewer free fine particles in the settled kaolin supernatant. This is because the presence of bulk nanobubbles results in fewer free kaolin particles, which can reduce the occurrence of pore blockage in the filter medium and thus lower the filtration resistance of the medium.

Figure 9 shows the comparative distribution curves of the transverse relaxation time of filter cakes, both in the absence and presence of bulk NBs, under a dosage of 6 mL CPAM. The filter cake exhibits a sharp independent peak around 100 ms, indicating that the water in the filter cake formed by kaolin filtration mainly exists in the form of free water. This is consistent with the experimental results of Feng, et al. [70]. Furthermore, the presence of bulk NBs can decrease the free water content compared to that of without bulk NBs. The presence of bulk NBs could potentially facilitate the formation of fine pores, thereby enhancing the dewatering efficiency.

The flocculation and filtration of kaolin are very complex processes. This article provides preliminary evidence that the presence of bulk nanobubbles can act as a flocculant to a certain extent, which is beneficial for the flocculation and filtration of kaolin. Further research is needed in the future to investigate the effects of bulk nanobubbles on the flocculation kinetics of kaolin and the formation of filter cake pores during the filtration process.

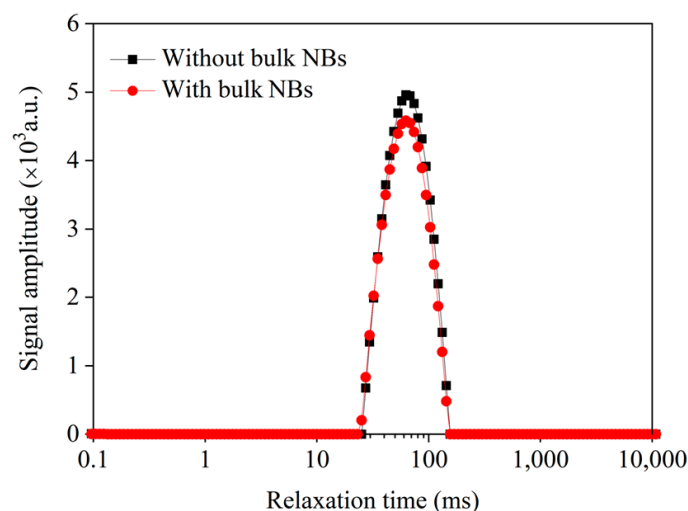


Figure 9. Comparisons of distribution curves of transverse relaxation time of filter cakes in the absence and presence of bulk NBs under 6 mL CPAM dosage.

4. Conclusions

This study is the first to investigate the impact of bulk NBs and flocculants on the flocculation and filtration characteristics of kaolin. The primary way in which bulk NBs affect the filtration process of kaolin is through the dispersion characteristics of CPAM. The study's main findings are as follows: (1) Bulk NBs can increase the settling rate by forming larger flocs, which reduces the electrostatic double-layer repulsion force; (2) With the appropriate CPAM dosage, bulk NBs can decrease the moisture content of the filter cake by forming looser structures and larger flocs, leading to a reduction in the filter cake's strength; (3) Bulk NBs can enhance the filtration characteristics of kaolin by decreasing the medium resistance (from 4.0×10^{-8} to 3.6×10^{-8}) and the specific cake resistance (from 8.3×10^{-9} to 7.6×10^{-9}), and by promoting the formation of fine pores in the filter cake. It is important to note that interactions between NBs, kaolin particles, and CPAM molecules can occur. Further research is needed to comprehensively study these interactions and to investigate the effects of bulk NBs on the flocculation, sedimentation, and filtration processes of kaolin in the future.

Author Contributions: Y.L.: methodology, software, validation, investigation, writing—original draft, writing—review and editing; G.M.: methodology, investigation, formal analysis, funding acquisition, writing—original draft, writing—review and editing; M.B.: methodology, data curation, project administration, writing—original draft, writing—review and editing; J.S.: Writing—review and editing, resources, supervision; X.B.: conceptualization, visualization, project administration, funding acquisition, writing—original draft, writing—review and editing. All authors have read and agreed to the published version of the manuscript.

Funding: This research was funded by the Natural Science Foundation of Shandong Province (Grant No. ZR2023QE103) the National Natural Science Foundation of China (52204296).

Data Availability Statement: The data presented in this study are available on request from the corresponding author.

Acknowledgments: The authors wish to sincerely thank Shaoqi Zhou for his valuable contributions to this work.

Conflicts of Interest: The authors declare no conflicts of interest. In addition, Yihong Li and Jie Sha were employed by the Shaanxi Xinneng Coal Preparation Technology Co., Ltd. The remaining authors declare that the research was conducted in the absence of any commercial or financial relationships that could be construed as a potential conflict of interest.

References

1. Fernandez, R.; Martirena, F.; Scrivener, K.L. The origin of the pozzolanic activity of calcined clay minerals: A comparison between kaolinite, illite and montmorillonite. *Cem. Concr. Res.* **2011**, *41*, 113–122. [[CrossRef](#)]
2. Ramos, J.J.; Leiva, W.H.; Castillo, C.N.; Ihle, C.F.; Fawell, P.D.; Jeldres, R.I. Seawater flocculation of clay-based mining tailings: Impact of calcium and magnesium precipitation. *Miner. Eng.* **2020**, *154*, 106417. [[CrossRef](#)]
3. Sun, X.; Chen, Z.; Guo, K.; Fei, J.; Dong, Z.; Xiong, H. Geopolymeric flocculation-solidification of tail slurry of shield tunnelling spoil after sand separation. *Constr. Build. Mater.* **2023**, *374*, 130954. [[CrossRef](#)]
4. Liu, D.; Edraki, M.; Fawell, P.; Berry, L. Improved water recovery: A review of clay-rich tailings and saline water interactions. *Powder Technol.* **2020**, *364*, 604–621. [[CrossRef](#)]
5. Lagaly, G.; Ziesmer, S. Colloid chemistry of clay minerals: The coagulation of montmorillonite dispersions. *Adv. Colloid Interface Sci.* **2003**, *100–102*, 105–128. [[CrossRef](#)]
6. Lee, K.E.; Teng, T.T.; Morad, N.; Poh, B.T.; Hong, Y.F. Flocculation of kaolin in water using novel calcium chloride-polyacrylamide (CaCl₂-PAM) hybrid polymer. *Sep. Purif. Technol.* **2010**, *75*, 346–351. [[CrossRef](#)]
7. Agmo Hernández, V. An overview of surface forces and the DLVO theory. *ChemTexts* **2023**, *9*, 10. [[CrossRef](#)]
8. Mishchuk, N.A.; Marinin, A.I.; Marchenko, A.M. Coagulation, Sedimentation, and Consolidation of Aqueous Clay Dispersions. *J. Water Chem. Technol.* **2020**, *42*, 8–15. [[CrossRef](#)]
9. Lee, C.S.; Robinson, J.; Chong, M.F. A review on application of flocculants in wastewater treatment. *Process Saf. Environ. Prot.* **2014**, *92*, 489–508. [[CrossRef](#)]
10. Zhang, Y.; Hu, S.; Yang, X.; Jiang, F.; Wu, C.; Li, J.; Liu, K. Performance and mechanism of polyacrylamide stabilizers in coal water slurry. *Colloid Surf. A-Physicochem. Eng. Asp.* **2021**, *630*, 127544. [[CrossRef](#)]
11. Zhao, C.; Zhou, J.; Yan, Y.; Yang, L.; Xing, G.; Li, H.; Wu, P.; Wang, M.; Zheng, H. Application of coagulation/flocculation in oily wastewater treatment: A review. *Sci. Total Environ.* **2021**, *765*, 142795. [[CrossRef](#)]
12. Yang, R.; Li, H.; Huang, M.; Yang, H.; Li, A. A review on chitosan-based flocculants and their applications in water treatment. *Water Res.* **2016**, *95*, 59–89. [[CrossRef](#)]
13. Nazari, B.; Abdolalian, S.; Taghavijelouidar, M. An environmentally friendly approach for industrial wastewater treatment and bio-adsorption of heavy metals using Pistacia soft shell (PSS) through flocculation-adsorption process. *Environ. Res.* **2023**, *235*, 116595. [[CrossRef](#)]
14. You, L.; Lu, F.; Li, D.; Qiao, Z.; Yin, Y. Preparation and flocculation properties of cationic starch/chitosan crosslinking-copolymer. *J. Hazard. Mater.* **2009**, *172*, 38–45. [[CrossRef](#)]
15. Tian, D.; Xie, H.-Q. Synthesis and Flocculation Characteristics of Konjac Glucomannan-g-Polyacrylamide. *Polym. Bull.* **2008**, *61*, 277–285. [[CrossRef](#)]
16. Gao, Y.; Li, Q.; Shi, Y.; Cha, R. Preparation and Application of Cationic Modified Cellulose Fibrils as a Papermaking Additive. *Int. J. Polym. Sci.* **2016**, *2016*, 6978434. [[CrossRef](#)]
17. Li, H.; Cai, T.; Yuan, B.; Li, R.; Yang, H.; Li, A. Flocculation of Both Kaolin and Hematite Suspensions Using the Starch-Based Flocculants and Their Floc Properties. *Ind. Eng. Chem. Res.* **2015**, *54*, 59–67. [[CrossRef](#)]
18. Wang, J.-P.; Chen, Y.-Z.; Yuan, S.-J.; Sheng, G.-P.; Yu, H.-Q. Synthesis and characterization of a novel cationic chitosan-based flocculant with a high water-solubility for pulp mill wastewater treatment. *Water Res.* **2009**, *43*, 5267–5275. [[CrossRef](#)]
19. Shabanizadeh, H.; Taghavijelouidar, M. Potential of pomegranate seed powder as a novel natural flocculant for pulp and paper wastewater treatment: Characterization, comparison and combination with alum. *Process Saf. Environ. Prot.* **2023**, *170*, 1217–1227. [[CrossRef](#)]
20. Shabanizadeh, H.; Taghavijelouidar, M. A sustainable approach for industrial wastewater treatment using pomegranate seeds in flocculation-coagulation process: Optimization of COD and turbidity removal by response surface methodology (RSM). *J. Water Process. Eng.* **2023**, *53*, 103651. [[CrossRef](#)]
21. Zhang, L.; Min, F.; Chen, J.; Wang, L.; Zhu, Y.; Ren, B. Study on flocculation performance and mechanism of cationic polyacrylamide on montmorillonite: Insights from experiments and molecular simulations. *Chem. Phys.* **2024**, *579*, 112190. [[CrossRef](#)]
22. Zhou, S.; Bu, X.; Alheshibri, M.; Zhan, H.; Xie, G. Floc structure and dewatering performance of kaolin treated with cationic polyacrylamide degraded by hydrodynamic cavitation. *Chem. Eng. Commun.* **2022**, *209*, 798–807. [[CrossRef](#)]
23. Taghavijelouidar, M.; Yaqoubnejad, P.; Ahangar, A.K.; Rezaia, S. A rapid, efficient and eco-friendly approach for simultaneous biomass harvesting and bioproducts extraction from microalgae: Dual flocculation between cationic surfactants and bio-polymer. *Sci. Total Environ.* **2023**, *854*, 158717. [[CrossRef](#)]
24. Liu, Z.; Huang, M.; Li, A.; Yang, H. Flocculation and antimicrobial properties of a cationized starch. *Water Res.* **2017**, *119*, 57–66. [[CrossRef](#)]
25. Ding, S.; Zou, H.; Zhou, S.; Bu, X.; Bilal, M.; Wang, X. The preparation of hydroxypropyl starch grafted acrylamide and its enhancement on flocculation of coal slime water. *Energy Sources Part A-Recovery Util. Environ. Eff.* **2022**, *44*, 7934–7948. [[CrossRef](#)]
26. Ding, S.; Pan, F.; Zhou, S.; Bu, X.; Alheshibri, M. Ultrasonic-assisted flocculation and sedimentation of coal slime water using the Taguchi method. *Energy Sources Part A-Recovery Util. Environ. Eff.* **2023**, *45*, 10523–10536. [[CrossRef](#)]
27. Su, Y.; Du, H.; Huo, Y.; Xu, Y.; Wang, J.; Wang, L.; Zhao, S.; Xiong, S. Characterization of cationic starch flocculants synthesized by dry process with ball milling activating method. *Int. J. Biol. Macromol.* **2016**, *87*, 34–40. [[CrossRef](#)]

28. Yang, Z.; Wu, H.; Yuan, B.; Huang, M.; Yang, H.; Li, A.; Bai, J.; Cheng, R. Synthesis of amphoteric starch-based grafting flocculants for flocculation of both positively and negatively charged colloidal contaminants from water. *Chem. Eng. J.* **2014**, *244*, 209–217. [[CrossRef](#)]
29. Wei, H.; Gao, B.; Ren, J.; Li, A.; Yang, H. Coagulation/flocculation in dewatering of sludge: A review. *Water Res.* **2018**, *143*, 608–631. [[CrossRef](#)] [[PubMed](#)]
30. Xu, S.; Shi, J.; Deng, J.; Sun, H.; Wu, J.; Ye, Z. Flocculation and dewatering of the Kaolin slurry treated by single- and dual-polymer flocculants. *Chemosphere* **2023**, *328*, 138445. [[CrossRef](#)] [[PubMed](#)]
31. Lemanowicz, M.; Kus, A.; Gierczycki, A.T. Influence of ultrasonic conditioning of flocculant on the aggregation process in a tank with turbine mixer. *Chem. Eng. Process.* **2010**, *49*, 205–211. [[CrossRef](#)]
32. Chistyakova, G.V.; Koksharov, S.A.; Vladimirova, T.V. Dependence of the solubility of atmospheric oxygen in weakly alkaline aqueous solutions on surfactant concentration. *Russ. J. Phys. Chem. A* **2012**, *86*, 1753–1755. [[CrossRef](#)]
33. Zhou, S.; Wang, X.; Bu, X.; Wang, M.; An, B.; Shao, H.; Ni, C.; Peng, Y.; Xie, G. A novel flotation technique combining carrier flotation and cavitation bubbles to enhance separation efficiency of ultra-fine particles. *Ultrason. Sonochem.* **2020**, *64*, 105005. [[CrossRef](#)]
34. Zhang, F.; Sun, L.; Yang, H.; Gui, X.; Schönherr, H.; Kappl, M.; Cao, Y.; Xing, Y. Recent advances for understanding the role of nanobubbles in particles flotation. *Adv. Colloid Interface Sci.* **2021**, *291*, 102403. [[CrossRef](#)]
35. Etchepare, R.; Oliveira, H.; Nicknig, M.; Azevedo, A.; Rubio, J. Nanobubbles: Generation using a multiphase pump, properties and features in flotation. *Miner. Eng.* **2017**, *112*, 19–26. [[CrossRef](#)]
36. Bu, X.; Zhou, S.; Tian, X.; Ni, C.; Nazari, S.; Alheshibri, M. Effect of aging time, airflow rate, and nonionic surfactants on the surface tension of bulk nanobubbles water. *J. Mol. Liq.* **2022**, *359*, 119274. [[CrossRef](#)]
37. Zhou, S.; Li, Y.; Nazari, S.; Bu, X.; Hassanzadeh, A.; Ni, C.; He, Y.; Xie, G. An Assessment of the Role of Combined Bulk Micro- and Nano-Bubbles in Quartz Flotation. *Minerals* **2022**, *12*, 944. [[CrossRef](#)]
38. Bu, X.; Alheshibri, M. The effect of ultrasound on bulk and surface nanobubbles: A review of the current status. *Ultrason. Sonochem.* **2021**, *76*, 105629. [[CrossRef](#)]
39. Alheshibri, M.; Qian, J.; Jehannin, M.; Craig, V.S.J. A History of Nanobubbles. *Langmuir* **2016**, *32*, 11086–11100. [[CrossRef](#)] [[PubMed](#)]
40. Zhou, S.; Nazari, S.; Hassanzadeh, A.; Bu, X.; Ni, C.; Peng, Y.; Xie, G.; He, Y. The effect of preparation time and aeration rate on the properties of bulk micro-nanobubble water using hydrodynamic cavitation. *Ultrason. Sonochem.* **2022**, *84*, 105965. [[CrossRef](#)] [[PubMed](#)]
41. Tao, D. Recent advances in fundamentals and applications of nanobubble enhanced froth flotation: A review. *Miner. Eng.* **2022**, *183*, 107554. [[CrossRef](#)]
42. Diniz, P.H.V.; Azevedo, A.C.; Rubio, J. Filtration of fine mineral particles assisted by nanobubbles. *Miner. Eng.* **2023**, *204*, 108428. [[CrossRef](#)]
43. Li, P.; Zhang, M.; Lei, W.; Yao, W.; Fan, R. Effect of Nanobubbles on the Slime Coating of Kaolinite in Coal Flotation. *ACS Omega* **2020**, *5*, 24773–24779. [[CrossRef](#)] [[PubMed](#)]
44. Lei, W.; Zhang, M.; Zhang, Z.; Zhan, N.; Fan, R. Effect of bulk nanobubbles on the entrainment of kaolinite particles in flotation. *Powder Technol.* **2020**, *362*, 84–89. [[CrossRef](#)]
45. Žbik, M.; Horn, R.G. Hydrophobic attraction may contribute to aqueous flocculation of clays. *Colloid Surf. A-Physicochem. Eng. Asp.* **2003**, *222*, 323–328. [[CrossRef](#)]
46. Zhou, S.; Bu, X.; Wang, X.; Ni, C.; Ma, G.; Sun, Y.; Xie, G.; Bilal, M.; Alheshibri, M.; Hassanzadeh, A.; et al. Effects of surface roughness on the hydrophilic particles-air bubble attachment. *J. Mater. Res. Technol.-JMRT* **2022**, *18*, 3884–3893. [[CrossRef](#)]
47. Wu, C.; Wang, L.; Harbottle, D.; Masliyah, J.; Xu, Z. Studying bubble-particle interactions by zeta potential distribution analysis. *J. Colloid Interface Sci.* **2015**, *449*, 399–408. [[CrossRef](#)] [[PubMed](#)]
48. Huang, K.; Yoon, R.-H. Control of bubble ζ -potentials to improve the kinetics of bubble-particle interactions. *Miner. Eng.* **2020**, *151*, 106295. [[CrossRef](#)]
49. Fan, X.; Zhang, Z.; Li, G.; Rowson, N.A. Attachment of solid particles to air bubbles in surfactant-free aqueous solutions. *Chem. Eng. J.* **2004**, *59*, 2639–2645. [[CrossRef](#)]
50. Besra, L.; Sengupta, D.K.; Roy, S.K. Particle characteristics and their influence on dewatering of kaolin, calcite and quartz suspensions. *Int. J. Miner. Process.* **2000**, *59*, 89–112. [[CrossRef](#)]
51. Gao, J.; Bu, X.; Zhou, S.; Wang, X.; Alheshibri, M.; Peng, Y.; Xie, G. Graphite flotation by β -cyclodextrin/kerosene Pickering emulsion as a novel collector. *Miner. Eng.* **2022**, *178*, 107412. [[CrossRef](#)]
52. Wang, X.; Shaoqi, Z.; Bu, X.; Ni, C.; Xie, G.; Peng, Y. Investigation on interaction behavior between coarse and fine particles in the coal flotation using focused beam reflectance measurement (FBRM) and particle video microscope (PVM). *Sep. Sci. Technol.* **2021**, *56*, 1418–1430. [[CrossRef](#)]
53. Ni, C.; Bu, X.; Xia, W.; Peng, Y.; Yu, H.; Xie, G. Observing slime-coating of fine minerals on the lump coal surface using particle vision and measurement. *Powder Technol.* **2018**, *339*, 434–439. [[CrossRef](#)]
54. Lu, J.; Yuan, Z.; Liu, J.; Li, L.; Zhu, S. Effects of magnetite on magnetic coating behavior in pentlandite and serpentine system. *Miner. Eng.* **2015**, *72*, 115–120. [[CrossRef](#)]

55. Dixon, D.V.; Soares, J.B.P. Molecular weight distribution effects of polyacrylamide flocculants on clay aggregate formation. *Colloid Surf. A-Physicochem. Eng. Asp.* **2022**, *649*, 129487. [[CrossRef](#)]
56. Li, S.; Wang, X.-M.; Zhang, Q.-L. Dynamic experiments on flocculation and sedimentation of argillized ultrafine tailings using fly-ash-based magnetic coagulant. *Trans. Nonferrous Met. Soc. China* **2016**, *26*, 1975–1984. [[CrossRef](#)]
57. Huo, W.; Zhang, X.; Gan, K.; Chen, Y.; Xu, J.; Yang, J. Effect of zeta potential on properties of foamed colloidal suspension. *J. Eur. Ceram. Soc.* **2019**, *39*, 574–583. [[CrossRef](#)]
58. Besra, L.; Sengupta, D.K.; Roy, S.K.; Ay, P. Flocculation and dewatering of kaolin suspensions in the presence of polyacrylamide and surfactants. *Int. J. Miner. Process.* **2002**, *66*, 203–232. [[CrossRef](#)]
59. Besra, L.; Sengupta, D.K.; Roy, S.K.; Ay, P. Influence of polymer adsorption and conformation on flocculation and dewatering of kaolin suspension. *Sep. Purif. Technol.* **2004**, *37*, 231–246. [[CrossRef](#)]
60. Besra, L.; Sengupta, D.K.; Roy, S.K.; Ay, P. Influence of surfactants on flocculation and dewatering of kaolin suspensions by cationic polyacrylamide (PAM-C) flocculant. *Sep. Purif. Technol.* **2003**, *30*, 251–264. [[CrossRef](#)]
61. Shao, H.; Chang, J.; Lu, Z.; Grundy, J.S.; Xie, G.; Xu, Z.; Liu, Q. Probing Interaction of Divalent Cations with Illite Basal Surfaces by Atomic Force Microscopy. *J. Phys. Chem. C* **2020**, *124*, 2079–2087. [[CrossRef](#)]
62. Hu, Y.; Liu, X. Chemical composition and surface property of kaolins. *Miner. Eng.* **2003**, *16*, 1279–1284. [[CrossRef](#)]
63. Takahashi, M. ζ Potential of Microbubbles in Aqueous Solutions: Electrical Properties of the Gas–Water Interface. *J. Phys. Chem. B* **2005**, *109*, 21858–21864. [[CrossRef](#)] [[PubMed](#)]
64. Bu, X.; Zhang, T.; Chen, Y.; Peng, Y.; Xie, G.; Wu, E. Comparison of mechanical flotation cell and cyclonic microbubble flotation column in terms of separation performance for fine graphite. *Physicochem. Probl. Miner. Process.* **2018**, *54*, 732–740.
65. Joglekar, A.; May, A.T. Product excellence through design of experiments. *Cereal Foods World* **1987**, *32*, 857–868.
66. Wang, X.; Bu, X.; Ni, C.; Zhou, S.; Yang, X.; Zhang, J.; Alheshibri, M.; Peng, Y.; Xie, G. Effect of scrubbing medium's particle size on scrubbing flotation performance and mineralogical characteristics of microcrystalline graphite. *Miner. Eng.* **2021**, *163*, 106766. [[CrossRef](#)]
67. Mao, Y.; Chen, Y.; Bu, X.; Xie, G. Effects of 20 kHz ultrasound on coal flotation: The roles of cavitation and acoustic radiation force. *Fuel* **2019**, *256*, 115938. [[CrossRef](#)]
68. Jones, A.N.; Bridgeman, J. Investigating the characteristic strength of flocs formed from crude and purified Hibiscus extracts in water treatment. *Water Res.* **2016**, *103*, 21–29. [[CrossRef](#)]
69. Amjad, H.; Khan, Z.; Tarabara, V.V. Fractal structure and permeability of membrane cake layers: Effect of coagulation–flocculation and settling as pretreatment steps. *Sep. Purif. Technol.* **2015**, *143*, 40–51. [[CrossRef](#)]
70. Feng, Z.; Dong, X.; Chen, R. The relationship between permeability and pore structure of coal slime filter cake based on fractal characteristics. *Coal Sci. Technol.* **2023**, *51*, 312–322.

Disclaimer/Publisher's Note: The statements, opinions and data contained in all publications are solely those of the individual author(s) and contributor(s) and not of MDPI and/or the editor(s). MDPI and/or the editor(s) disclaim responsibility for any injury to people or property resulting from any ideas, methods, instructions or products referred to in the content.